Available online at www.sciencedirect.com
ScienceDirect
Atmospheric Environment 42 (2008) 3468–3490
ATMOSPHERIC ENVIRONMENT
www.elsevier.com/locate/atmosenv

MICS-Asia II: The model intercomparison study for Asia Phase II methodology and overview of findings

G.R. Carmichael[a,*], T. Sakurai[b], D. Streets[c], Y. Hozumi[b], H. Ueda[b], S.U. Park[d], C. Fung[e], Z. Han[b], M. Kajino[f], M. Engardt[g], C. Bennet[g], H. Hayami[h], K. Sartelet[i], T. Holloway[j], Z. Wang[k], A. Kannari[l], J. Fu[m], K. Matsuda[n], N. Thongboonchoo[a], M. Amann[o]

[a]*Center for Global and Regional Environmental Research, University of Iowa, IA, USA*
[b]*Acid Deposition and Oxidant Research Center, Niigata, Japan*
[c]*Argonne National Laboratory, IL, USA*
[d]*Seoul National University, Seoul, South Korea*
[e]*Hong Kong Environmental Protection Department, Hong Kong SAR, China*
[f]*Disaster Prevention Research Institute, Kyoto University, Kyoto, Japan*
[g]*Swedish Meteorological and Hydrological Institute, Norrkoping, Sweden*
[h]*Central Research Institute of Electric Power Industry, Chiba, Japan*
[i]*Centre d'Enseignement et de Recherche en Environnement Atmospherique, Marne la Vallée, France*
[j]*Center for Sustainability and the Global Environment, University of Wisconsin-Madison, WI, USA*
[k]*Institute of Atmospheric Physics, Beijing, China*
[l]*Independent Researcher, Tokyo, Japan*
[m]*The University of Tennessee, TN, USA*
[n]*Meisei University, Tokyo, Japan*
[o]*International Institute for Applied System Analysis Laxenburg, Austria*

Received 2 March 2007; accepted 4 April 2007

Abstract

Results from the Model Intercomparison Study Asia Phase II (MICS-Asia II) are presented. Nine different regional modeling groups simulated chemistry and transport of ozone (O_3), secondary aerosol, acid deposition, and associated precursors, using common emissions and boundary conditions derived from a global model. Four-month-long periods, representing 2 years and three seasons (i.e., March, July, and December in 2001, and March in 2002), are analyzed. New observational data, obtained under the EANET (the Acid Deposition Monitoring Network in East Asia) monitoring program, were made available for this study, and these data provide a regional database to compare with model simulations. The analysis focused around seven subject areas: O_3 and related precursors, aerosols, acid deposition, global inflow of pollutants and precursor to Asia, model sensitivities to aerosol parameterization, analysis of emission fields, and detailed analyses of individual models, each of which is presented in a companion paper in this issue of *Atmospheric*

*Corresponding author.
E-mail address: gcarmich@engineering.uiowa.edu (G.R. Carmichael).

1352-2310/$ - see front matter
doi:10.1016/j.atmosenv.2007.04.007

Environment. This overview discusses the major findings of the study, as well as information on common emissions, meteorological conditions, and observations.

Keywords: Air quality modeling; Asia air quality; Ozone; Aerosol composition

1. Introduction

The long-range transport and fate of pollutants in the atmosphere is an area of increasing scientific interest and political concern. It is now well established that pollution levels at a specific location can be the result of both nearby and distant sources. Chemical transport models (CTMs) have become critical tools in the analysis of the fate and transport of emissions. While significant advances in CTMs have taken place, predicting air quality remains a challenging problem due to the complex processes occurring at widely different scales and by their strong coupling across scales. Air quality predictions also have large uncertainties associated with: incomplete and/or inaccurate emissions information, lack of key measurements to impose initial and boundary conditions, physical and chemical processes missing from the model, and poorly parameterized processes.

In order to help develop a better common understanding of the performance and uncertainties of CTMs in East Asia applications, a model intercomparison study on long-range transport and deposition of sulfur, i.e., Model Intercomparison Study Asia Phase I (MICS-Asia Phase I), was carried out during the period from 1998 to 2002. Eight models participated in the Phase I study (Carmichael et al., 2001, 2002). Each conducted simulations under similar conditions and model results were compared with observations. A primary focus of this study was to better understand the capabilities of regional models in predicting source–receptor (S/R) relationships for sulfur deposition in East Asia. In the early to mid-1990s, regional models for acid deposition were just beginning to be applied in Asia and early results indicated significant differences in calculated S/R relationships between different groups (cf. Carmichael et al., 2002 and references therein; Ichikawa and Fujita, 1995). The MICS-Asia study was initiated to help understand these differences and to better understand how to model long-range transport in East Asia. Model results for the periods January and May 1993 were intercompared. S/R relationships estimated by the models showed a high degree of consistency in identifying the main S/R relationships, as well as in the relative contributions of wet/dry pathways for removal. But at some locations estimated deposition amounts were found to vary by a factor of 5. The influences of model structure and parameters on model performance were evaluated. The S/R relationships were found to be most sensitive to uncertainties in the sulfur emission inventory, and secondarily to the driving meteorology. Both the factors were found to be more important than the uncertainties in the model parameters for wet removal and sulfate production. A major limitation of this study was the lack of coherent data sets of sulfur ambient concentrations and deposition measurements over East Asia upon which to evaluate model performance.

In 2003, this initiative was expanded to include nitrogen compounds, O_3, and aerosols—key species for regional health and ecosystem protection, and pollutants of growing concern throughout Asia. This broader collaborative study—MICS-Asia Phase II—examined four different periods, encompassing two different years and three different seasons (i.e., March, July, and December in 2001, and March in 2002). An additional feature unique to Phase II is the inclusion of global inflow to the study domain. Furthermore, new observational data obtained under the EANET (the Acid Deposition Monitoring Network in East Asia) monitoring program were made available for this study, and these data provided a region-wide database to use in the comparisons. Nine different regional modeling groups simulated chemistry and transport of O_3, precursors, sulfur dioxide, and secondary aerosols, using common emissions (Streets et al., 2003c) and boundary conditions derived from the global model of ozone and related tracers (MOZART, v. 2.4). The analysis focused on subject areas identified a priori as deserving special attention, including O_3 and its precursors, aerosols, and acid deposition, as well as broader issues in global inflow to the study region, aerosol parameterization, and analysis of emission fields. The design of the experiments and the analysis were coordinated through annual meetings held at the International

Institute for Applied System Analysis (IIASA) located in Laxenburg, Austria, as well as additional coordination meetings.

In this paper, we present an overview of the study design, including a discussion of the emissions and meteorological fields used in the analysis. We also describe the observational data and analysis used in the study, and present some of the highlights of findings resulting from this study. In companion manuscripts, further details of the MICS-Asia Phase II (hereafter referred to as MICS-II) results are presented. Han et al. compare predictions of ozone and additional trace gases among the participating models, Hayami et al. discuss particulate sulfate, nitrate, and ammonium, and the results for acidic deposition are presented in Wang et al. In addition, the impacts of the global boundary conditions and imported emissions on the regional air quality predictions are discussed by Holloway et al., and the sensitivity of the aerosol predictions to various processes and parameterizations is described in Sartelet et al. An example of a detailed comparison of one of the participating models is presented by Fu et al. Finally to provide information concerning the reliability of the emissions data used in the intercomparison, the MICS-II inventory was compared with a detailed emission inventory for Japan (Kannari et al., 2008).

2. Intercomparison framework

The intercomparison study design follows the efforts of MICS-I. The participants were to utilize a common emissions data set and a common set of boundary conditions. Each modeling group was provided a common set of meteorological fields developed using the Penn State/UCAR Mesoscale Model v. 5 (MM5), but in fact all groups opted to use their own meteorological fields for the four study months. These inputs were distributed via publicly accessible websites and hard-drives shipped to participant groups (for the large meteorological data set). Following the completion of the modeling protocol, each group submitted specified fields to a common website. These results were converted to GrADS format for ease in comparison with each other, and with observational data.

2.1. Participating models

Results from nine modeling groups using three-dimensional Eulerian models were analyzed in MICS-II. These included: a model from Seoul National University (Chang and Park, 2004); the PATH model from Hong Kong Environmental Protection Department; the RAQM model from Acid Deposition and Oxidant Research Center, Japan (Han et al., 2004); the MSSP model from Disaster Prevention Research Institute, Kyoto University (Kajino et al., 2004); the STEM model from Center of Global and Regional Environmental Research (CGRER), Iowa University (Carmichael et al., 2003); the MATCH model from Swedish Meteorological and Hydrological Institute (Engardt, 2000); the Polair3D model from CEREA (Centre d'Enseignement et de Recherche en Environnement Atmospherique), France (Boutahar et al., 2004); and two applications of the CMAQ model (http://www.epa.gov/asmdnerl/CMAQ/), one by Central Research Institute of Electric Power Industry, Japan, and the other by the University of Tennessee, USA (Fu et al., this issue).

Table 1 presents some basic information on the structure of each model. These models differ in the chemical mechanisms used, the detail of aerosol processes, as well as in coordinate systems and numerical schemes. They compose an excellent set of representative approaches to air quality modeling. For analysis purposes, the study team decided not to identify the models by name. From this point on, the models are referred to by their assigned numbers (i.e., M-1 to M-9).

The full Asia domain shown in Fig. 1 was used in the preparation of emissions and baseline meteorology. Participant models differed in the extent of the region included in the simulation (Fig. 1), so detailed intercomparison of the models was limited to the subdomain common to all the participating models (shown in Fig. 1 as M-3/M-4 domain). Also shown in Fig. 1 are the monitoring stations used for this study. Most stations are located in the common domain, with a few additional sites in Southeast Asia and Russia. Seven of the nine models used common monthly mean boundary conditions from a global CTM (MOZART-2). Each model used its own meteorological fields, which were derived through three ways. Most models used the MM5 model (Grell et al., 1994) for meteorology (M1, M2, M3, M4, M7, M8, and M9), but with some differences in the usage of reanalysis data (Table 1) and options. M5 used RAMS (Pielke et al., 1992) with ECWMF reanalysis to generate its meteorological fields, whereas M6 directly ingested ECWMF data with the same resolution (0.5°) as that in the CTM.

Table 1
Overview of the models that participated in the MIC-II study

	Grid number	Grid size	Met. fields	Boundary data	Dry deposition	Wet deposition
M-1	145 × 195	45 km	MM5/NCEP	MOZART-II	Wesely (1989)	Seinfeld (1986)
M-2	143 × 133	40.5 km	MM5/ECMWF	MOZART-II	Wesely (1989)	RADM (Chang et al., 1987)
M-3	110 × 60	0.5°	MM5/GANAL[a]	MOZART-II	Wesely (1989)	RADM
M-4	110 × 60	0.5°	MM5/NCEP	MOZART-II	Wesely (1989)	Henry's Law
M-5	90 × 60	0.5°	RAMS/ECMF	Original	Wesely (1989)	Fixed rate
M-6	166 × 134	0.5°	ECMWF	MOZART-II	Engardt (2000)	Berge (1993)
M-7	166 × 144	45 km	MM5/GANAL[a]	MOZART-II	Wesely (1989)	RADM
M-8	121 × 61	45 km	MM5/GANAL[a]	MOZART-II	Wesely (1989)	Sportisse and DuBoi (2002)
M-9	164 × 97	36 km	MM5/NCEP	GEOS-Chem	Wesely (1989)	Henry's Law

[a]GANAL: Global objective analysis data developed by Japan Meteorological Agency.

EANET Sites in 2002

ID	Site Name	Characteristics	Lat	Lon	Country
1	Guanyinqiao	Urban	29.6	106.5	China
2	Jinyunshan	Rural	29.8	106.4	
3	Shizhan	Urban	34.2	109.0	
4	Weishuiyuan	Rural	34.4	108.9	
5	Jiwozi	Remote	33.8	108.8	
6	Hongwen	Urban	24.5	118.1	
7	Xiaoping	Remote	24.9	118.0	
8	Xiang-Zhou	Urban	22.3	113.6	
9	Zhuxian-Cavern	Urban	22.2	113.5	
10	Jakarta	Urban	6.2	106.8	Indonesia
11	Serpong	Rural	6.3	106.6	
12	Kototabang	Remote	0.2	100.3	
13	Bandung	Urban	6.9	107.6	
14	Rishiri	Remote	45.1	141.2	Japan
15	Tappi	Remote	41.3	141.4	
16	Ogasawara	Remote	27.8	142.2	
17	Sado-seki	Remote	38.2	138.4	
18	Happo	Remote	36.7	137.8	
19	Oki	Remote	36.3	133.2	
20	Yusuhara	Remote	33.4	132.9	
21	Hedo	Remote	26.9	128.3	
22	Ijira	Rural	35.7	136.7	
23	Banryu	Urban	34.7	131.8	
24	Petaling-Jaya	Urban	3.1	101.7	Malaysia
25	Tanah-Rata	Remote	4.5	101.4	
26	Ulaanbaatar	Urban	47.9	106.8	Mongolia
27	Terelj	Remote	48.0	107.5	
28	Metro-Manila	Urban	14.6	121.1	Philippines
29	Los-Banos	Rural	14.2	121.3	
30	Kanghwa	Rural	37.7	126.3	Republic of Korea
31	Cheju	Remote	33.3	126.2	
32	Imsil	Rural	35.6	127.2	
33	Mondy	Remote	51.7	101.0	Russia
34	Listvyanka	Rural	51.9	104.9	
35	Irkutsk	Urban	52.2	104.3	
36	Primorskaya	Rural	43.7	132.1	
37	Bangkok	Urban	13.8	100.5	Thailand
38	Samutprakarn	Urban	13.7	100.6	
39	Patumthani	Rural	14.0	100.8	
40	Vachiralongkorn-Dam	Remote	14.8	98.6	
41	Mae-Hia	Rural	18.8	98.9	
42	Hanoi	Urban	21.0	105.9	Vietnam
43	Hoa-Binh	Rural	20.8	105.3	

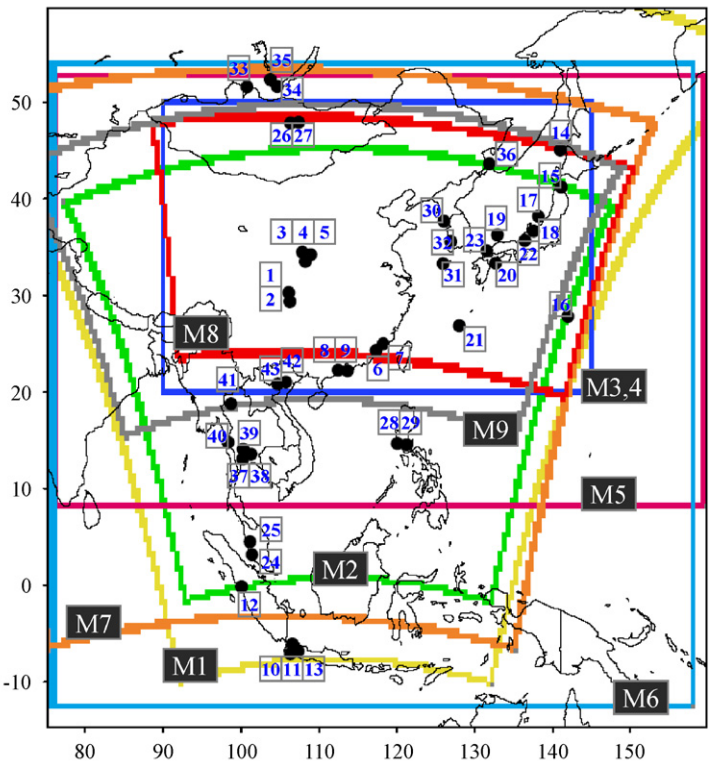

Fig. 1. The MICS-II study domain. Shown are the domains used by the individual models (described in Table 1). Also shown are the EANET observation locations used in the study.

The 4-month-long periods selected for analysis (i.e., March, July, and December in 2001, and March in 2002) cover a range of atmospheric conditions. March 2001 was a period of high dust transport and high volcanic emissions. July and December 2001 provided examples of a summer period with warm and high precipitation conditions, and a winter period with cold and low precipitation

conditions, respectively. These periods provide contrasts between primary and secondary pollution levels. March 2002 provided an opportunity to compare results for the same month for two different years. The 2001–2002 period was selected to take advantage of the emissions prepared for the TRACE-P research campaigns and the rich observational databases provided by both the TRACE-P and ACE-Asia campaigns.

2.2. Emissions

Common emissions were prepared for the intercomparison study for sulfur dioxide (SO_2), nitrogen oxides (NO_x), carbon monoxide (CO), total particulate matter (PM_{10} and $PM_{2.5}$), black carbon (BC), organic carbon (OC), ammonia (NH_3), methane (CH_4), and non-methane volatile organic compounds (NMVOC) from anthropogenic sources (area sources and SO_2 point sources), biomass burning, and volcanos, aggregated on a grid with 0.5° resolution. Some models (M3, M4, M5, M6) operated on the same grid as the emissions were available on, while others had to interpolate the gridded emissions to their internal grid. The release heights for elevated sources were prescribed at an altitude of 300 m for large point sources and 1500 m for volcanic emission. Natural emissions (biogenic NMVOC, soil and lightning NO_x, dust and sea salt) were not prescribed and left up to the different modeling groups. For anthropogenic emissions, the TRACE-P inventory (Streets et al., 2003a), which was developed for the year 2000, was modified to reflect the four selected study periods by including growth in the period 2000–2001 and to 2002, and considering intraannual monthly variation of emissions as described below.

2.2.1. Anthropogenic emissions

The 2000 TRACE-P inventory (Streets et al., 2003a) provides monthly emissions of the major species throughout the MICS-II domain. In China, seasonality is influenced most significantly by higher emissions during the winter heating season and the greater intensity of evaporative emissions during warmer months. These monthly variation profiles were applied to emissions of four of the relevant species for MICS-II: SO_2, NO_x, NMVOC, and NH_3. In addition, projected growth in emissions of these four species from 2000 to 2001 and 2002 for China (the dominate source region) was estimated using appropriate sector- and fuel-specific factors from the China Statistical Yearbooks, 2000–2003. The results are shown in Fig. 2. These figures show the emissions for the various periods, separately disaggregated for three major regions: Northern China, Central China, and Southern China. Table 2 summarizes the changes relative to the averaged year-2000 emissions.

Some significant growth trends are predicted for this period on the basis of fuel-use changes and changes in other activity parameters. The increase in SO_2 emissions shown in Table 2 is not, however, consistent with official Chinese estimates of SO_2 emissions in the period 2000–2002, which are essentially flat. (A large increase occurs later, in 2003.) Coal use increased substantially in this period, according to the statistics, so it is unclear whether the Chinese data are incorrect, or whether they incorporate reductions in the average sulfur content of coal or sulfur removal efficiency. The SO_2 changes shown in Table 2 should be viewed cautiously, as they may error on the high side. The growth in emissions of NO_x and NMVOC are reasonable, as they reflect the increase in vehicle traffic and use of petroleum products. In all cases, except for NH_3/December 2001, projected emissions are higher than the TRACE-P values. For December 2001, NH_3 emissions may be significantly smaller (25%) than in the TRACE-P average, and this is expected to be manifested mostly in Southern China.

2.2.2. Volcanic SO_2 emissions

Volcanic emissions played a large role in sulfur emissions during this period of study. Of special importance to this study is the fact that Mt. Oyama on Miyakejima Island (Miyakejima volcano: 139.53°E, 34.08°N, 813 m MSL), located in the northwest Pacific Ocean, 180 km south of Tokyo metropolitan area, began to erupt on 8 July 2000, and has emitted huge amounts of SO_2 since then (Kajino et al., 2004). The Seismological and Volcanological Department of the Japan Meteorological Agency (SVD-JMA) has performed continuous measurements of the SO_2 emissions and smoke height above the crater since September 2000, 2 months after the beginning of the eruption (Kazahaya, 2001). Table 3 shows the SO_2 emissions and plume height during the four MICS-II periods. In March 2001, the eruption was still quite intense. SO_2 emissions were 27,350 tons day^{-1} on average, with a maximum of 45,900 tons day^{-1} and with a larger standard deviation than during the other

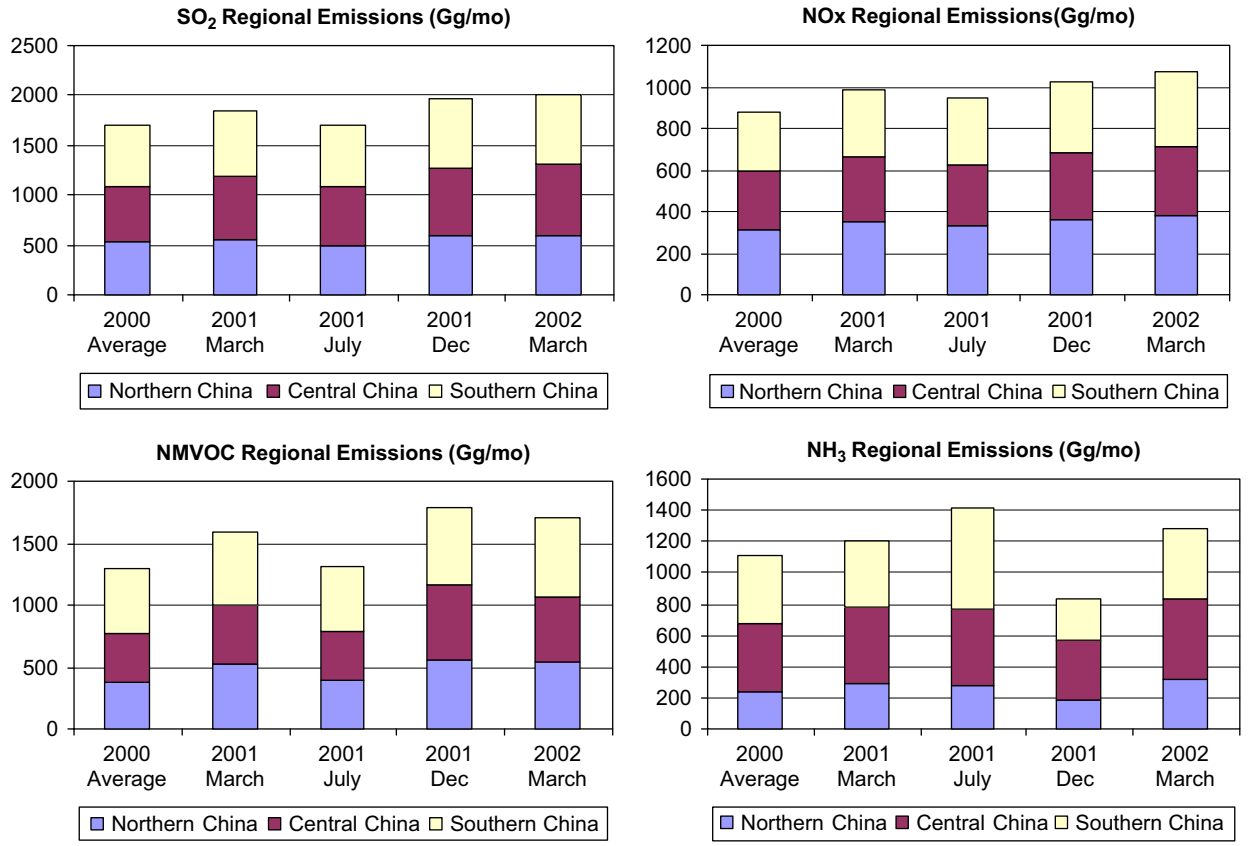

Fig. 2. Estimated changes in anthropogenic emission between the TRACE-P inventory and the four MICS-II analysis months for SO_2, NO_x, NMVOC, and NH_3.

Table 2
Differences in anthropogenic emissions relative to the year-2000 TRACE-P average (%)

	March 2001	July 2001	December 2001	March 2002
NO_x	12.3	7.8	16.5	22.5
SO_2	8.9	0.9	15.8	19.2
NMVOC	22.8	1.2	38.9	31.4
NH_3	8.3	26.7	−25.4	15.9

periods. The SO_2 emissions decreased with time but increased again in March 2002. Smoke height varies from 100 to 2000 m and the average, maximum, and standard deviation decreased over time.

2.2.3. *Biomass burning emissions*

Monthly data sets of biomass burning emissions were provided for the model intercomparison runs. These reflected typical monthly profiles developed from analysis of AVHRR fire-counts in the period 1999–2000, applied to the TRACE-P estimate of typical annual biomass burning amounts by region (Woo et al., 2003; Streets et al., 2003b). However, it was necessary to perform some check to see if actual

Table 3
SO_2 emissions and smoke height of the Miyakejima volcanic eruption during the MICS periods, with values of average, standard deviation, minimum, maximum, and median

	March 2001	July 2001	December 2001	March 2002
SO_2 emission (tons day^{-1})				
Ave	27,350	14,611	12,960	15,875
Stdev	12,585	3476.5	2659.0	6266.5
Min	12,100	10,100	9000	6900
Max	45,900	21,600	19,200	23,400
Med	24,850	13,400	13,050	18,350
Smoke height (m)				
Ave	758.7	563.8	481.0	446.1
Stdev	427.7	297.0	309.7	246.3
Min	100	100	100	100
Max	2000	1600	1700	1200
Med	700	500	400	400

burning in the months analyzed was larger or smaller than expected. As a qualitative check, monthly global fire maps were downloaded from the ATSR World Fire Atlas (European Space Agency). Results were found to be typical, and show no unexpected features. In March 2001, Asian burning was restricted to Southeast Asia (severe) and isolated areas of eastern China (perhaps land clearing). In July 2001, fires in northern Siberia were widespread, affecting the most northerly part of the MICS-II domain. During the same month, very little burning occurred in Southeast Asia and only in a few isolated areas in eastern China. In December 2001, there was essentially no biomass burning occurring in this part of Asia. In March 2002, as in March 2001, there was again extensive burning in Southeast Asia and only very isolated burning spots in eastern China. We conclude that biomass burning in these four months was quite typical and will be reasonably represented by the emission profiles provided in the TRACE-P inventory.

2.2.4. Emission evaluation

To provide preliminary information concerning the reliability of the standard emissions data, the MICS-II inventory was compared with a high-resolution emission inventory for Japan, EA-Grid2000-Japan. Although these inventories are based upon different estimation methodologies, it was found that regional emissions are consistent, with differences smaller than 10% for SO_2, NO_x, and NMVOC, and smaller than 30% for CO and NH_3. Differences in emission amounts for all species were smaller than the 95% confidence intervals estimated for the MICS-II emissions data. The gridded emissions ($0.5^\circ \times 0.5^\circ$) were evaluated and the two inventories matched well for NO_x, NMVOC, CO, and $PM_{2.5}$, even though the spatial allocation techniques for the local inventory were much more detailed. For SO_2 emissions, the differences in the grid-based inventories were greater. Although some emission problems still remain, such as diurnal variations that are not considered in the MICS-II emission data, the comparison of the two estimates for Japan suggests that the MICS-II emissions data have appropriate properties for atmospheric model simulation over Japan. Further details are presented in Kannari et al. (2008).

2.3. General boundary conditions

Boundary conditions were derived from the simulation results of MOZART v. 2.4 according to each model domain. MOZART is a global scale model of atmospheric chemistry and transport, developed by the Atmospheric Chemistry Division (ACD) of the National Center for Atmospheric Research (NCAR), along with the National Oceanic and Atmospheric Administration (NOAA), Geophysical Fluid Dynamics Laboratory (GFDL), the Max Planck Institute (MPI) for Meteorology, and Princeton University. While this version of the model also includes select aerosol species, the gas phase mechanism is identical to that described in Horowitz et al. (2003).

To generate the boundary conditions distributed for use in MICS-II, the model was run with $2.8^\circ \times 2.8^\circ$ resolution, 34 vertical levels in hybrid-sigma coordinates, and meteorology from the NCAR Community Climate Model v. 2 (CCM-2). As with other climate models that do not employ assimilation of observed data, the CCM-2 meteorology reflects climatologically representative conditions, but no particular year. Boundary conditions were distributed for 11 species: CO, BC, OC, SO_2, nitrogen dioxide (NO_2), O_3, sulfate, ammonium nitrate, ethane, propane, and acetone. Ethane, propane, and acetone were selected as longer-lived hydrocarbons where long-range transport may play a role in calculating O_3 concentrations. To facilitate the input of boundary conditions into the MICS-II participant models, only monthly mean values were provided (rather than hourly or daily varying values).

Of the nine models participating in MICS-II, M-1, M-2, M-3, M-4, M-6, M-7, and M-8 used MOZART lateral boundary conditions. Of these, M-1 and M-3 used MOZART-derived upper boundary conditions for O_3 as well. M-6 interpolated the MOZART lateral O_3 values across the top of the domain, whereas M-7 and M-8 used a no-flux top boundary condition. M-5 used lateral boundary conditions derived from aircraft measurements taking during the TRACE-P campaign, and diagnosed the O_3 upper boundary condition from potential vorticity. The input of global boundary conditions into each model differs in details, leading to considerable differences in input fluxes from outside of the domain as discussed in Holloway et al. (2008).

2.4. Observation data

The model predictions were compared to the observational data from EANET. Historically, the

availability of consistent, reliable measurement data has been a bottleneck in the analysis of acid deposition and air quality throughout the Asia region. To address this need, EANET was initiated in 1998, following the model of the Co-operative Programme for Monitoring and Evaluation of the Long-range Transmission of Air Pollutants in Europe (EMEP). There are currently 47 wet deposition monitoring sites, located in 12 countries, with each country managing its own sites. All sites are operated using common quality assurance/quality control (QA/QC) standards promoted by the Acid Deposition and Oxidant Research Center (ADORC) which is designated as the Network Center for EANET. To advance regional understanding of the mechanisms underlying these observed patterns, EANET supported the current activities MICS-II, in collaboration with the IIASA, and participating groups.

Fig. 1 shows the location of EANET monitoring sites in 2002 for wet deposition and air concentrations used for model validation. Each monitoring site is classified into Urban (Ur), Rural (Ru) and Remote (Re) sites by regulations described in the guidelines (EANET, 2000). According to the latest EANET data report in 2005 (EANET, 2006), the 47 monitoring sites are located in East Asian region: 17 urban sites, 12 rural sites, and 18 remote sites. Wet deposition monitoring was conducted at all sites. Wet-only samplers were installed at all of the sites, and sampling collection was conducted on a daily basis at 30 sites, a weekly basis at 12 sites, and an event basis at 5 sites. Air concentration monitoring was conducted at 35 sites. Filter-pack monitors were installed at 30 sites in Indonesia, Japan, Malaysia, Mongolia, Philippines, Republic of Korea, Russia, Thailand, and Viet Nam, providing samples every one or two weeks. All sites provided concentration and deposition measurements as monthly mean values; daily concentrations were also available at 22 sites in China, Japan, Republic of Korea, Russia, and Thailand using automatic monitors. The data used in the various model comparisions are reported in EANET data reports (EANET, 2001, 2002, 2003).

In addition to the data provided from EANET, daily observational data for March 2001 monitored by Hayami (2005) in Fukue Island, Japan, were used. Fukue is located between Japan and Korea and surrounded by no large emissions. $PM_{2.5}$ was collected for chemical analysis by an impactor/denuder/filter-pack sampling system. An impactor was used to cut off particles larger than $PM_{2.5}$, and the denuder was used to collect gaseous species.

Aircraft observational data obtained by the TRACE-P experiment (Jacob et al., 2003) were also used. TRACE-P was conducted in the western Pacific in March–April 2001, with the aim to characterize the chemical composition and evolution of Asian outflow. In total, four flights (Flights 12, 13, 15 of DC-8 and Flight 13 of P-3B) were selected for use in the comparisons, all of which were associated with frontal lifting. In addition, observations from the Japan Meteorological Agency ozonsonde network were also used.

2.5. Analysis methodology

Analysis of regional model simulations was carried out by working groups established from the participants (see http://www.adorc.gr.jp/adorc/mics.html for details). Each modeling group supplied the requested fields for their model domain. For each domain, a common set of plots was prepared using the same projection and scales. The following predicted fields were analyzed for each of the four study periods:

(1) Monthly mean concentrations of gas phase SO_2, NO, NO_2, HNO_3, PAN, NH_3, O_3, aerosol and precipitation concentrations of sulfate, nitrate, and ammonium, for near surface 300, 1500, 3000, and 6000 m above ground level surfaces.
(2) Monthly accumulated surface deposition amounts: dry deposition: SO_2, HNO_3, NH_3, O_3, and aerosol sulfate, nitrate, ammonium; wet deposition: sulfate, nitrate, ammonium, and precipitation amount.
(3) Meteorological fields of temperature, relative humidity (RH), zonal wind, and meredional wind for the five layers discussed above.

In addition, the following comparisons with observations were performed:

(4) The predicted monthly mean quantities described above were compared with observations at the EANET sites.
(5) Daily averaged concentrations predicted were compared to observations at 17 reference sites: Jinyunshan (Ru), Weishuiyuan (Ru), Hongwen (Ur), Xiang-Zhou (Ur), Rishiri (Re), Ogasawara

(Re), Sado-seki (Re), Happo (Re), Oki (Re), Hedo (Re), Tanah-Rata (Re), Terelj (Re), Los Banos (Ru), Cheju (Re), Mondy (Re), Samtprakarn (Ur), Hoa-binh (Ru).

(6) Additional special comparisons were conducted for selected periods. These included comparison with TRACE-P aircraft data, high-resolution aerosol measurements at Fukue, and ozonesonde profiles.

3. Meteorological overview

As noted previously, reference meteorological fields were prepared by Prof. Z. Wang using the MM5 model, but participants were allowed to employ their own meteorological fields for the specified periods. Here, we discuss the general meteorological characteristics of the study time periods based on the reference MICS-II MM5

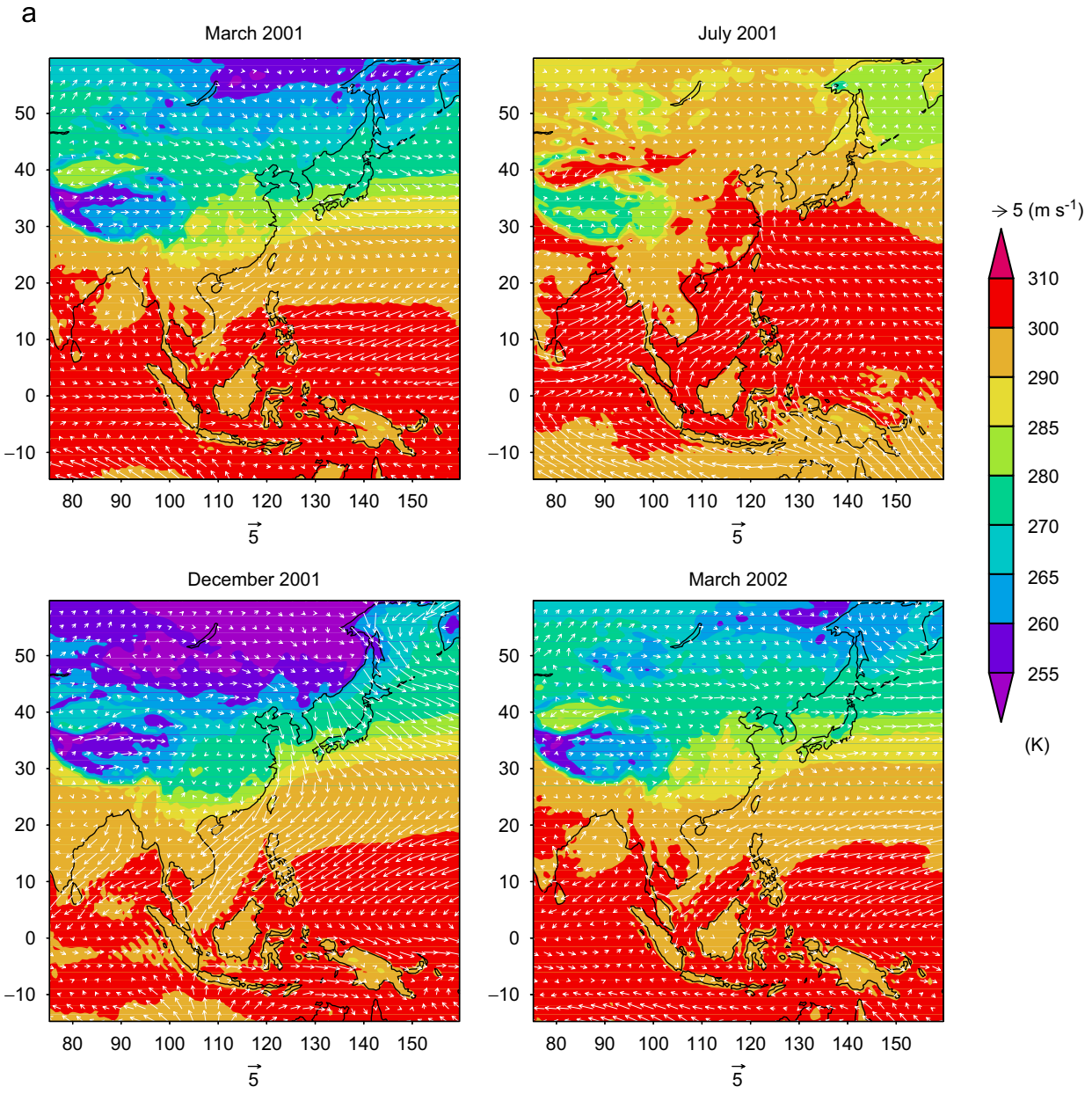

Fig. 3. Monthly mean distributions of temperature and horizontal winds at near surface (a) and at 3000 m above surface (b) for the four-month-long periods of study based on the MICS-II reference MM5 calculation.

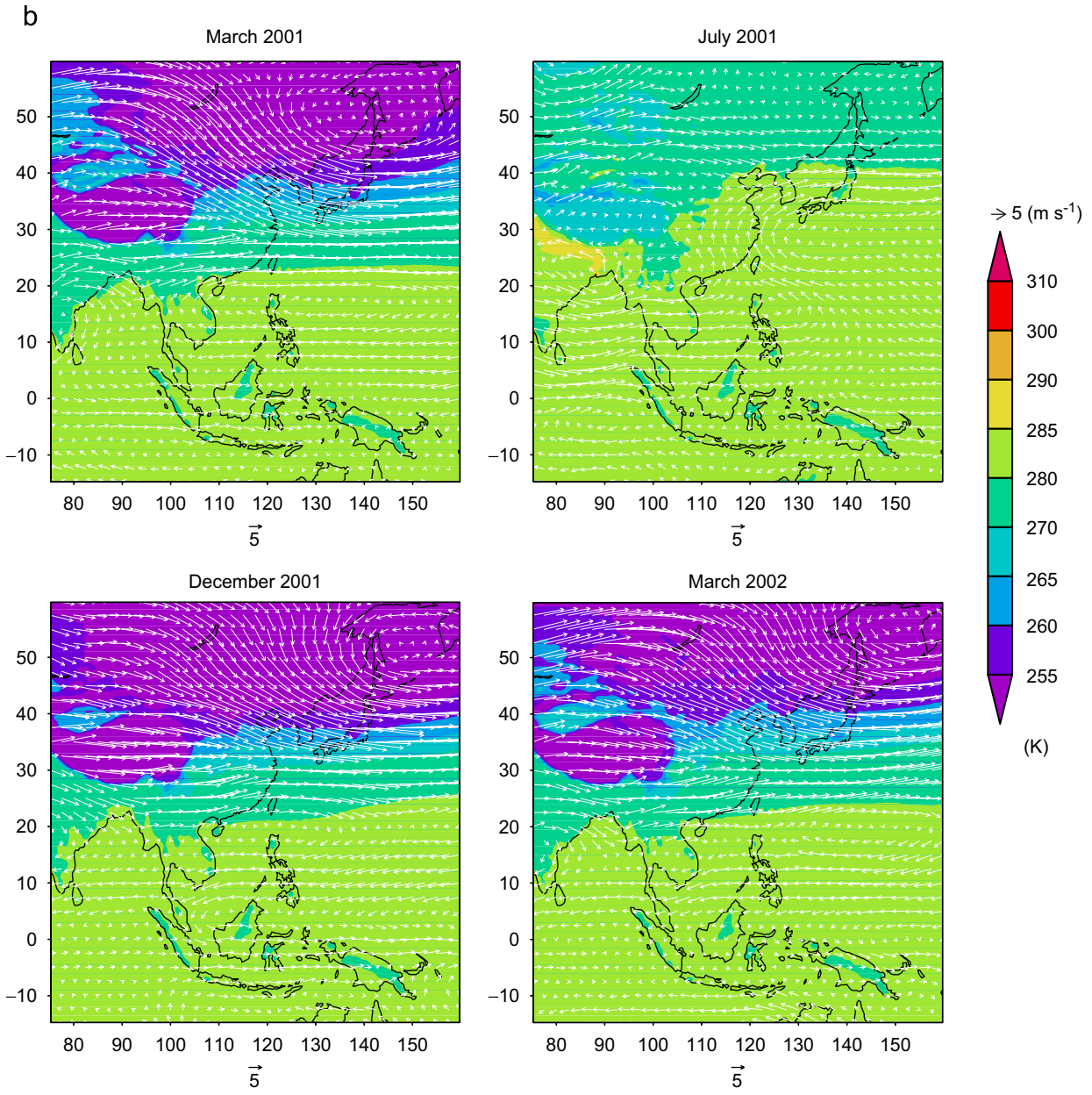

Fig. 3. (*Continued*)

simulations. We then compare the meteorological fields used by the different groups with observed meteorology.

3.1. General overview of meteorological conditions for the study periods

Monthly mean near surface temperature and wind vectors are shown in Fig. 3 and total precipitation is shown in Fig. 4. Both March periods were characterized by strong northwesterly winds over the mid-latitudes of eastern Asia, accompanied by frequent passages of cold fronts. Yellow sand events were observed several times in March 2001 and March 2002, with more events measured over Japan in 2002. In Southeast Asia, rainfall amounts were relatively light, although March 2001 showed heavier rainfall than usual in this region.

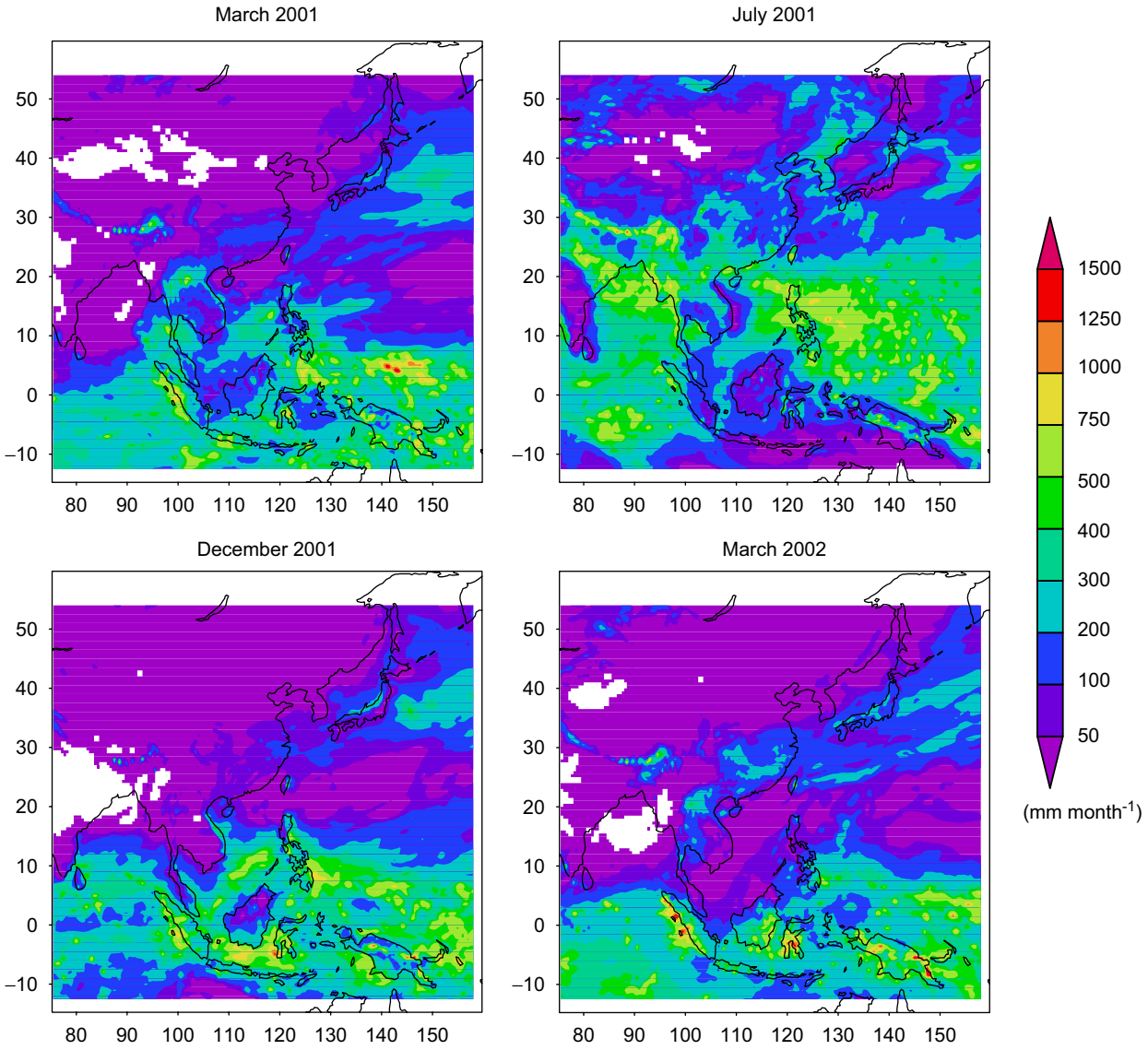

Fig. 4. Total accumulated monthly precipitation for the 4-month-long periods of study based on the MICS-II reference MM5 calculation.

Characteristic of typical summertime conditions, July shows warm temperatures and high levels of precipitation. Unusually high temperatures occurred in East Siberia, East China, and Japan. Southwesterly winds prevailed along the western Pacific Rim, resulting from the Subtropical Pacific High located to the southeast of Japan and the Continental Low over the Asian continent. Southerly winds persisted over the South China Sea as a result of the combination of the southwesterly monsoon and southeasterly trade winds from the Southern Hemisphere. High precipitation was found in Southern China, the South China Sea, and east of the Philippines. December is characterized by cold and low precipitation conditions. In December 2001, unusually low temperatures were observed in Mongolia, the western part of China, and the northern part of Japan. Rainfall amounts were larger than usual in the eastern part of China.

3.2. Comparison of modeled and observed meteorological fields

The predicted meteorology was evaluated against radiosonde observations over Japan at four sites (Naha, Yonago, Wajima, and Wakkanai). The performance

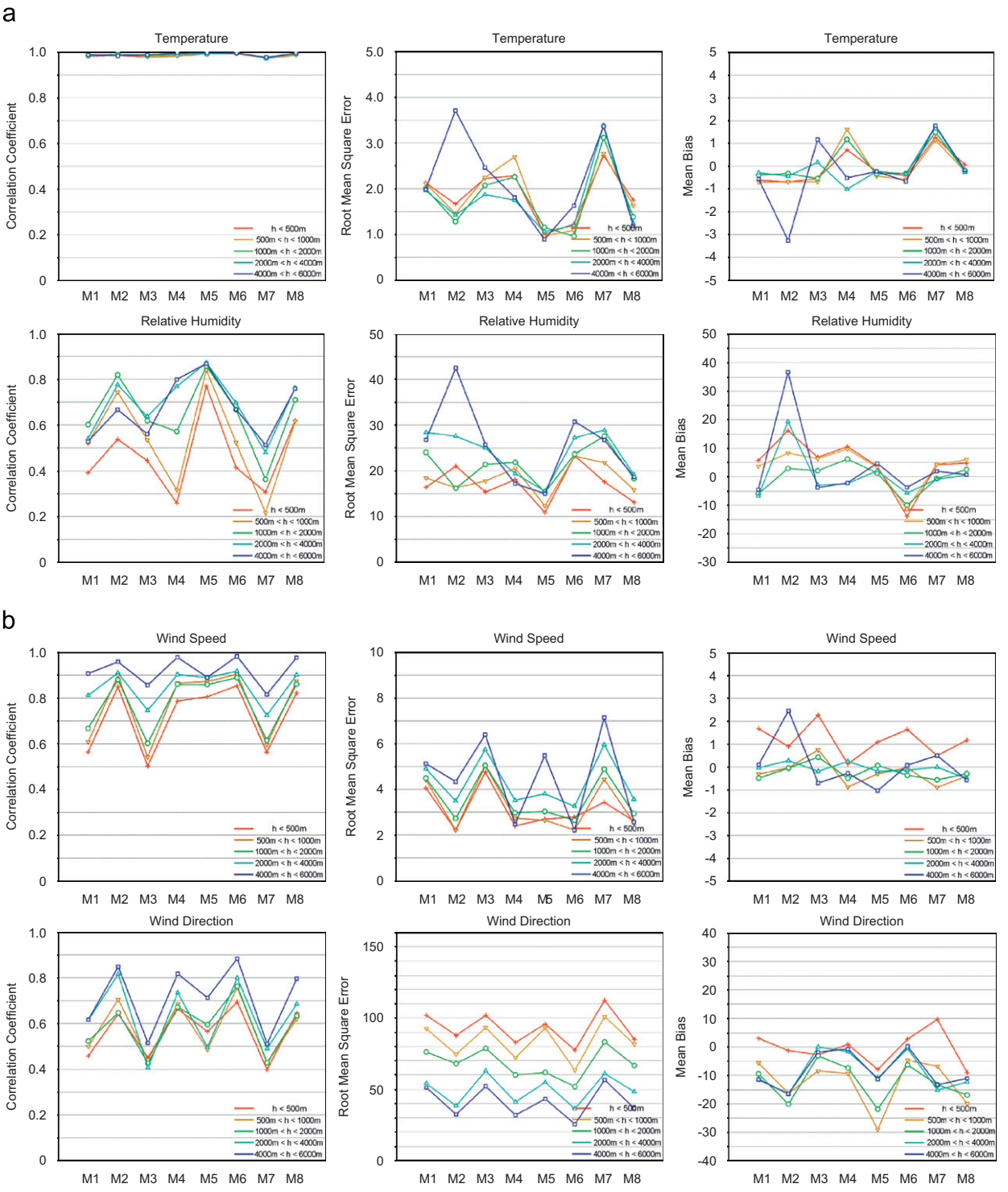

Fig. 5. Comparison of the predicted and observed (a) temperature and RH and (b) wind speed and direction. Observations are from radiosonde observations over Japan at four sites (Naha, Yonago, Wajima, and Wakkanai). The correlation coefficient, root mean square error, and mean bias at four altitudes are shown (values are for all four sets of sondings and all four months combined).

of the various models as a function of altitude is shown in Fig. 5, where the correlation coefficient, root mean square error, and mean bias at four altitudes for temperature, RH, wind speed, and direction (averaged over all four study months and all four sets of sondings) are presented. (Please note that not all individual modeling groups simulated all four periods or simulated all species; thus the number of model results presented in the figures represents the number of models that supplied results for that period.) Overall, temperature and wind speed are well represented by all the models, except in summer, where the performance of the models under conditions of relatively weak winds and frequent cyclone passings decreases. The correlation coefficients between predicted and measured temperature were greater than 0.98 for all models and bias errors within 1.0° for all seasons.

Wind direction and RH show lower predictive skill, with large differences in performance between altitudes. There are significant differences between models, but no systematic differences. The differences between model predictions reflect differences in parameterizations and analysis fields used (ECMWF, NCEP, GANAL) in the calculations. Differences are also related to differences in the horizontal and vertical resolutions of the models. It is interesting to note that M-6 used ECMWF data directly, while the others used mesoscale models to further process the meteorological fields (either MM5 or RAMS). In terms of these parameters, there is no clear difference between these models.

The characterization of the near surface meteorology is also important, and is needed to help interpret the differences between predicted and observed pollutant levels at ground-based measurement sites. The observed surface meteorology was obtained from the WMO surface network in Asia and used to evaluate predicted surface meteorology. Results comparing predictions of RH over a land area centered around Chongqing and a coastal region centered around Hong Kong are shown in Fig. 6. RH is an important parameter that plays a significant role in a variety of atmospheric chemistry, meteorology, and climate issues. For March 2001, the results show that the models are able to capture the synoptic temporal variability. Observed RH falls within the range of model values at Chongquing, an inland site, but all models show a persistent high bias in the coastal region of Hong Kong. These results help set the stage for the analysis of the pollutant comparisons. Since meteorology plays a key role in determining the pollution distributions resulting from a specific emissions distribution, errors in meteorology will propagate through to the pollutant distributions.

4. Results and discussions

The details of the results from the intercomparison analyses can be found in the individual MICS-II papers. Here we introduce some of the analysis and present some of the major features that have been identified through the intercomparison. Below

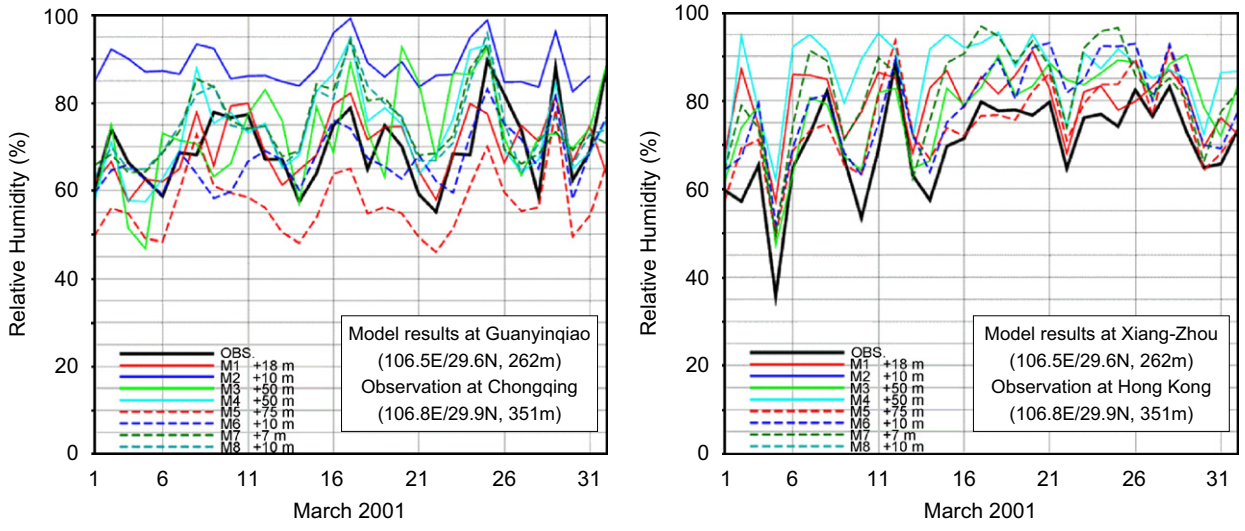

Fig. 6. Comparison of predicted and observed monthly mean surface RH over a land area centered around Chongqing and a coastal region centered around Hong Kong for March 2001. The height of the lowest model layer for each model is also given.

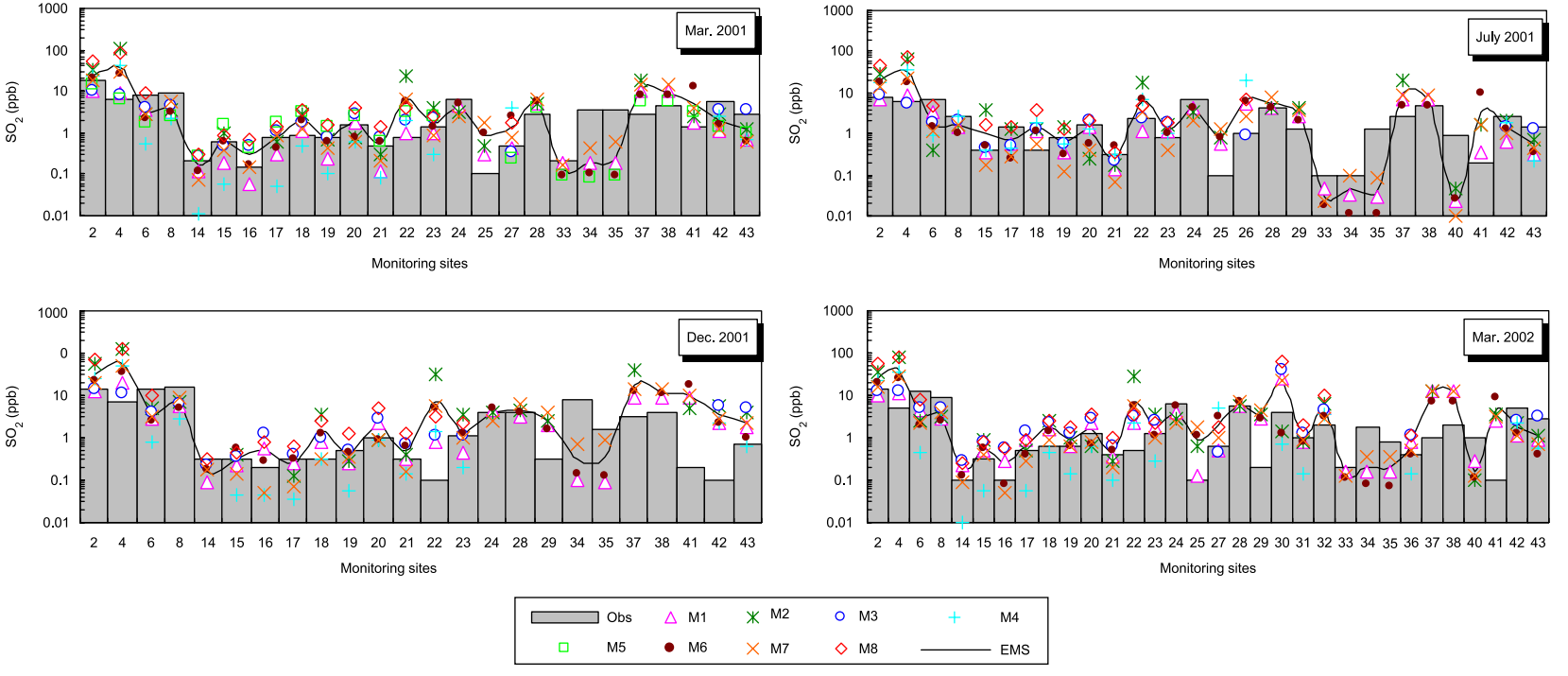

Fig. 7. Predicted and observed monthly mean near surface SO_2 concentrations. The locations of the observations sites are given in Fig. 1. Also shown is the ensemble mean prediction (EMS).

we restrict the discussion to the subdomain covered by all the models, i.e., 90°E–140°E, 20°N–50°N.

4.1. Sulfur distributions and deposition

Estimates of sulfur emissions in East Asia are believed to be more accurate than for any other species treated in MICS-II, due to long-term studies of air pollution and acid deposition in the region, and the strong dependence of sulfur emissions on the combustion of coal. Thus the comparison of predictions for sulfur compounds provides a benchmark for the intercomparison results. The prediction and observed monthly mean values of SO_2 for the 4 study months are shown in Fig. 7. In general, all models show good skill in simulating the SO_2 spatial variability, e.g., higher levels over China and moderate levels over Japan, which reflect the emission intensities in these regions. The models systematically overpredict observations at the Weishuiyuan site (site 4) of China and the Ijira site of Japan (site 22) for all months. This behavior probably reflects the rather coarse resolution of the models and resultant inability to distinguish the gradient for rural sites that may be located in or nearby grid cells containing large sulfur sources. The models systematically predict lower values at the sites in Russia (sites 33–35), due to the fact that Russian emissions were not included in the distributed emission inventory. Seasonal differences in SO_2 ambient levels are shown, with northern sites showing the highest values in the winter. There is also a strong seasonal cycle in the ambient levels in Southeast Asia (sites 37–43), where December values are lower than those in July. The models are not able to accurately capture the lower December values. Ensemble mean predictions (EMS; simple average of the models) were also calculated, and are also shown in the figure. In general, the intercomparison results show that the ensemble mean provides the most accurate prediction when compared to the various observations. Further details are presented in Han et al. (2008).

Fig. 8 shows the ensemble mean monthly averaged near-surface sulfate distribution for March 2001, along with the spatial distribution of the coefficient of variation. The coefficient of variation (hereinafter, CV) is defined as the standard deviation of the modeled fields divided by the average. The larger the value of CV, the lower the consistency among the models. As shown, mean concentrations of sulfate are high near Chongqing, Shanghai, and Seoul and in the volcanic plume from Mt. Miyake. In general, areas with relatively low CVs (below 0.5) are consistent with areas with concentrations over 6 $\mu g\,m^{-3}$, and high CVs are found in areas with low sulfate levels. The larger differences in model predictions away from emitting regions suggest differences associated with chemical processing and deposition of sulfate and SO_2. The northeast corner of the MICS-II domain has very

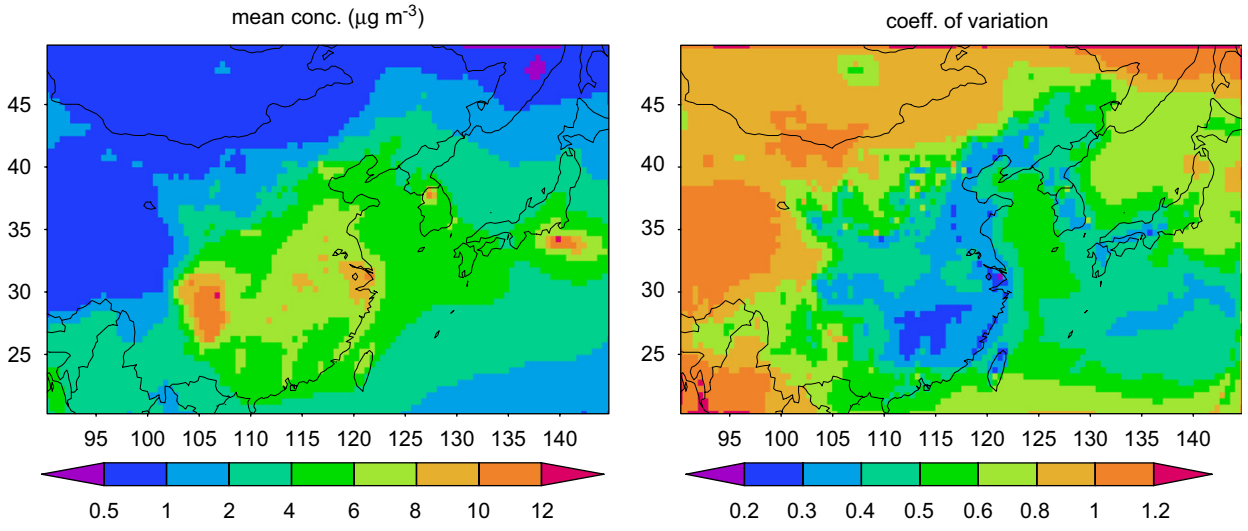

Fig. 8. The ensemble mean monthly averaged near-surface sulfate distribution for March 2001, along with the spatial distribution of the coefficient of variation. The coefficient of variation (CV) is defined as the standard deviation of the modeled fields divided by the average.

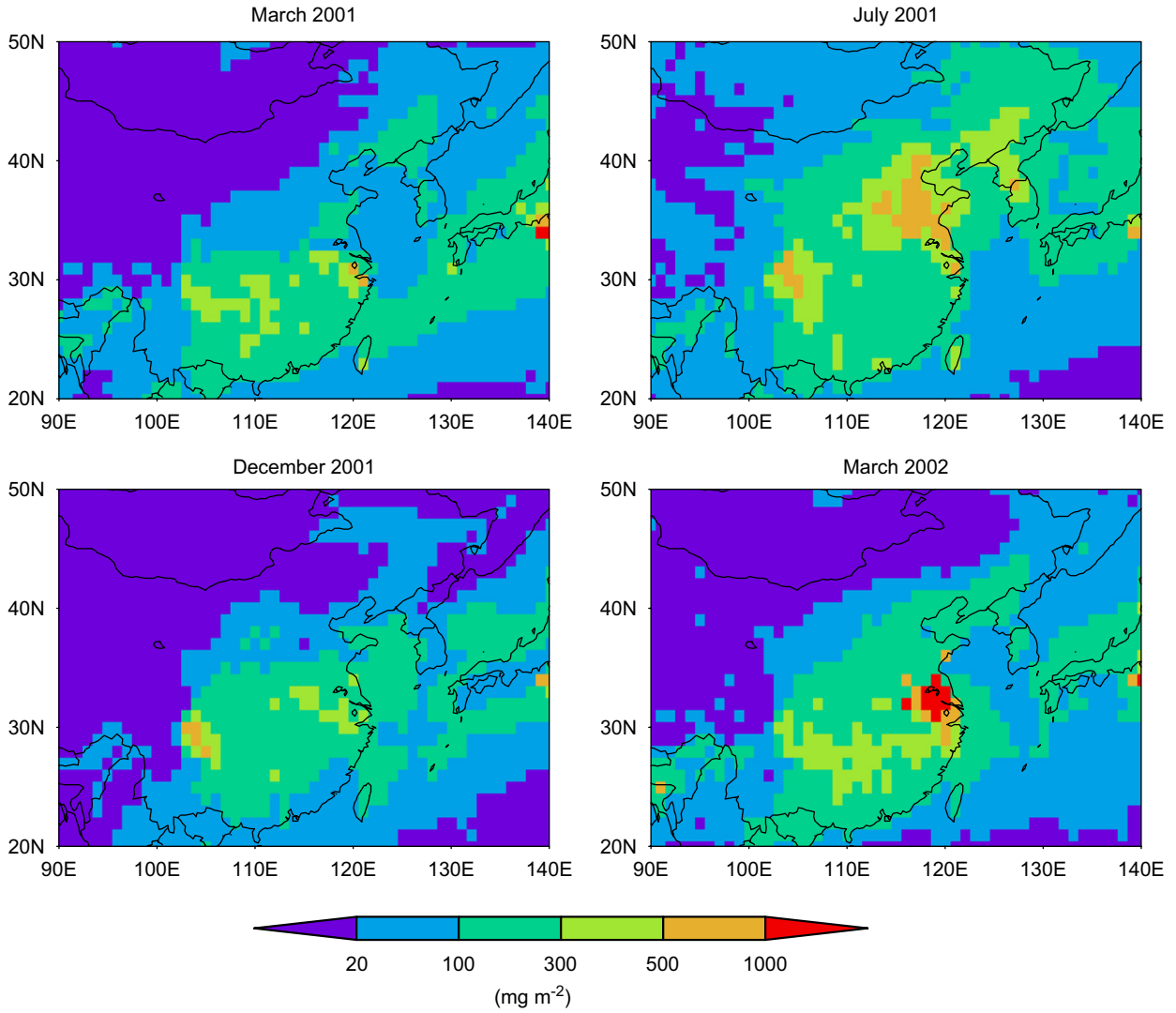

Fig. 9. The ensemble mean near surface monthly mean total sulfur deposition amounts (as sulfate) for the different seasons.

low sulfate concentrations, but of these concentrations, in March, over 50% of the sulfate in the northeast corner of the domain is due to European emissions, and over 10% on the eastern edge of the domain near 35°N is due to North American emissions (results based on the source-specific MOZART simulations discussed in Holloway et al., 2008). As discussed in Hayami et al. (2008), EMS agree well with measurements of sulfate and total ammonium. However, total nitrate is consistently underestimated. This underprediction was also found in the comparison of global model predictions (Dentener et al., 2006).

As part of MICS-II, the sensitivity of the predicted sulfate and nitrate aerosol concentrations to the different model treatments of the aerosol processes was investigated. Sensitivity studies were performed using different configurations of a reference aerosol module within a single CTM. The different configurations included different treatments of the size distribution (i.e., the number of sections), and physical processes (i.e., coagulation, condensation/evaporation, cloud chemistry, heterogeneous reactions, and sea-salt emissions). These results were compared to observations and to the results from the other MICS-II participating models. As discussed in Sartelet et al. (2008), the variability of predicted sulfate concentrations to aerosol module parameterizations was lower than the variability to the use of different

CTMs. However, for nitrate, the variability among the CTMs was of the same order of magnitude as the variability due to different aerosol parameterizations.

The ensemble mean total deposition of sulfur for the four periods is shown in Fig. 9. The total deposition of sulfur mainly occurs in Southern China, Japan, and the western Pacific in spring. In summer, high deposition regions move northward, where a deposition center is located in northern China, and another center in the southwest part of China. The highest values were predicted for March 2002, and they exceeded 1000 mg m^{-2} (as sulfate). The distribution of deposition of sulfur in winter is similar to spring. Wet deposition of sulfate and dry deposition of SO_2 are the two dominant modes of sulfur deposition.

The comparison of the monthly mean predicted and measured sulfate wet deposition for March and July 2001 is shown in Fig. 10. The observations generally reflect the spatial patterns shown in Fig. 9, with some regions showing higher sulfate wet deposition in March than in July (e.g., Oki, site 19), reflecting the fact that summertime flows at Oki are southerly, bringing marine air, while in the other seasons, the flows are from the west with high sulfur levels associated with this continental outflow. As shown, there can be large differences among the models for these two periods. The ensemble mean values at these sites are consistent

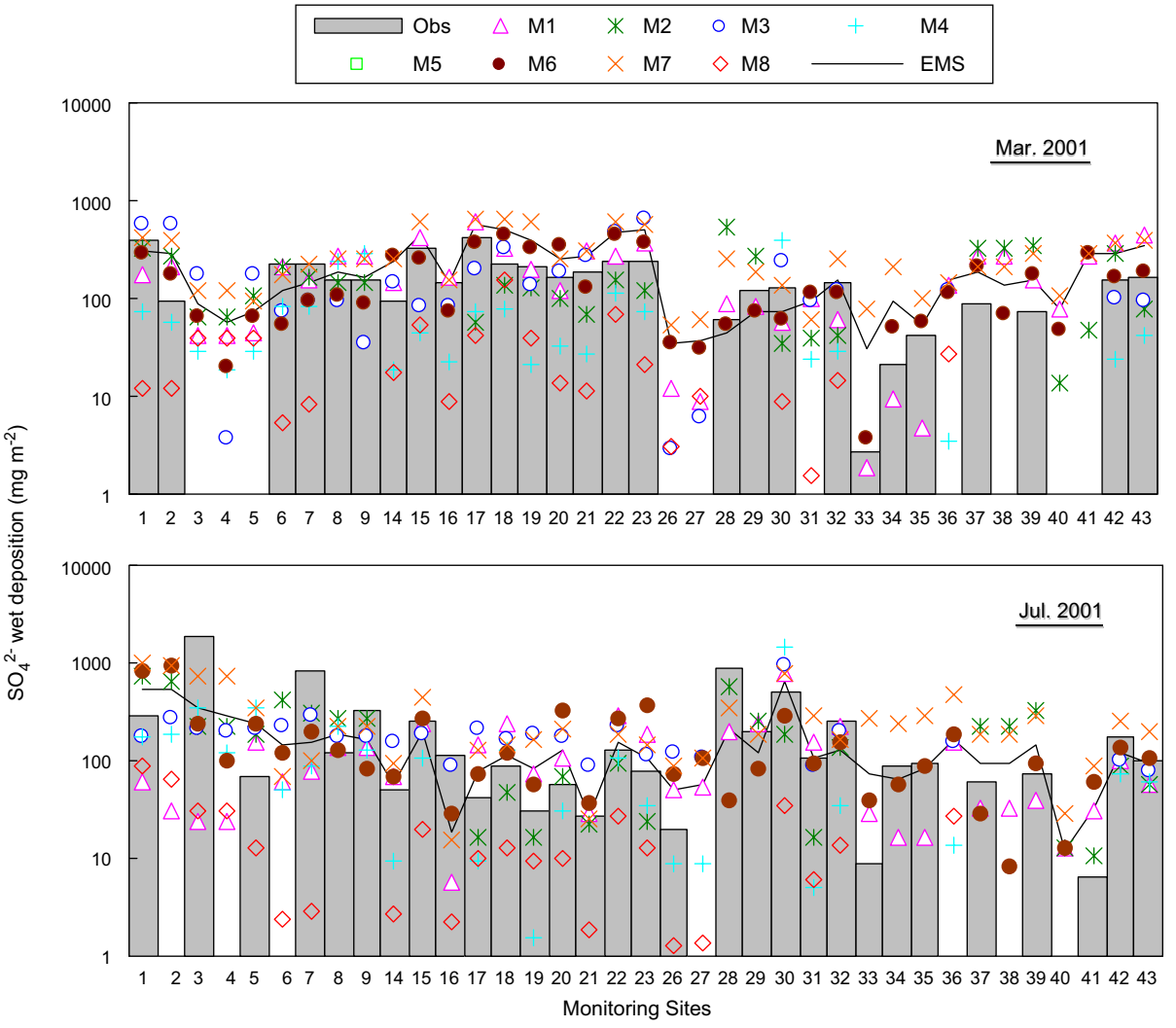

Fig. 10. The predicted and observed monthly mean sulfate wet deposition amounts (as sulfate) at various sites (see Fig. 1 for locations) for March and July 2001. Also shown is the ensemble mean predictions (EMS).

with observations, with a correlation coefficient of 0.73. Wang et al. (2008) further discusses sulfur deposition along with nitrate and ammonium deposition.

4.2. Ozone

Rising urban and regional O_3 concentrations pose a growing air pollution risk to health and vegetation in Asia. The inclusion of O_3 in MICS-II was an important advance from MICS-I. Regional models are being actively used to study O_3 in Asia, and MICS-II offered a valuable opportunity to compare these analysis tools. Furthermore, O_3 chemistry employs different precursors and mechanisms than sulfur chemistry, highlighting additional aspects of the model for evaluation, especially, VOC and NO_x emissions and photochemistry. The spatial distribution of MICS-II ensemble mean surface O_3 is presented in Fig. 11. It is important to note that there are significantly fewer measurement sites for O_3 in EANET than for acid deposition and acid-related species. In March and December, the mean distributions show a pronounced peak over Tibet in the western part of the domain, due to stratospheric O_3 affecting the high-altitude Tibetan Plateau. The O_3 values over this area are highest in March, topping 55 ppb. In July, a region of O_3 in excess of 40 ppb stretches across Northern China. In March and December, the regional-mean estimates show

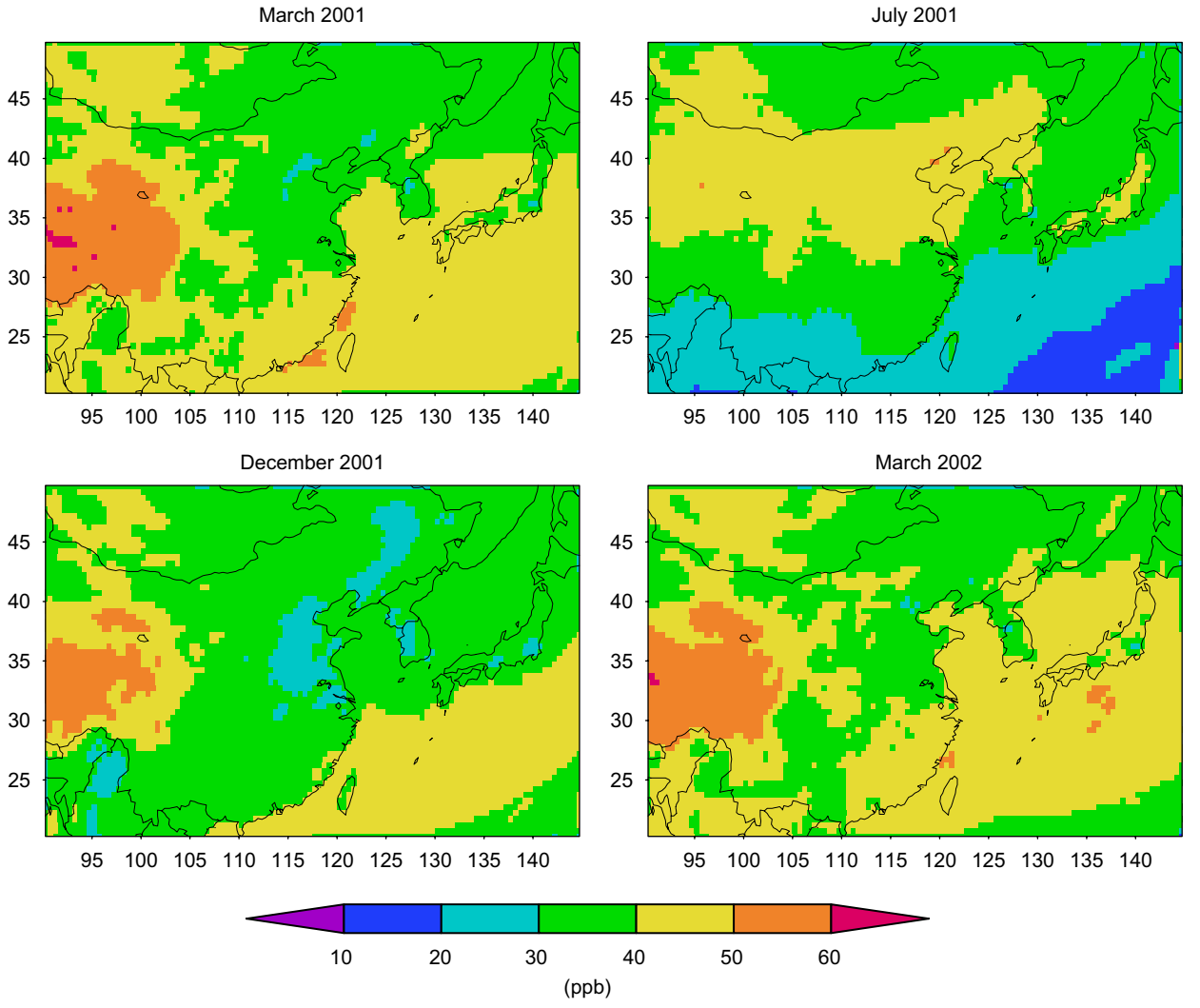

Fig. 11. The ensemble mean surface monthly mean ozone concentrations for the different seasons.

minimum O_3 values over northeast China and the Korean Peninsula. In March, these areas show typical concentrations of 40 ppb or lower. The O_3 distribution shows local minima in O_3 over large cities, and over Japan, reflecting titration due to high NO_x emissions. The mean fields for the two March periods are similar. In March and December, the O_3 concentrations over water are higher than the values at many inland locations in China. In contrast, continental concentrations during July greatly exceed oceanic values.

The CV of the O_3 predictions are presented in Fig. 12. In general, the values are low in the regions of elevated O_3, higher in the low concentration regions. Interestingly, the O_3 CVs are lower than those for sulfate. The highest values are found along the southern portion of the domain (i.e., over Southeast Asia). Differences in deposition or convection likely explain the cause of the high CV, but further study is needed to explain how these specific mechanisms differ among the models.

The comparison of predicted and observed monthly mean O_3 within the common domain is presented in Fig. 13. In general, the ensemble of predictions captures the observed variations within the regions (correlation coefficient of 0.6), although the predicted variations tend to be lower than that observed. Further details can be found in Han et al. (2008), where a detailed comparison of O_3 and its precursors is presented. The effect of boundary conditions on predicted O_3 and sulfate within the MICS-II domain is discussed in detail in Holloway et al. (2008).

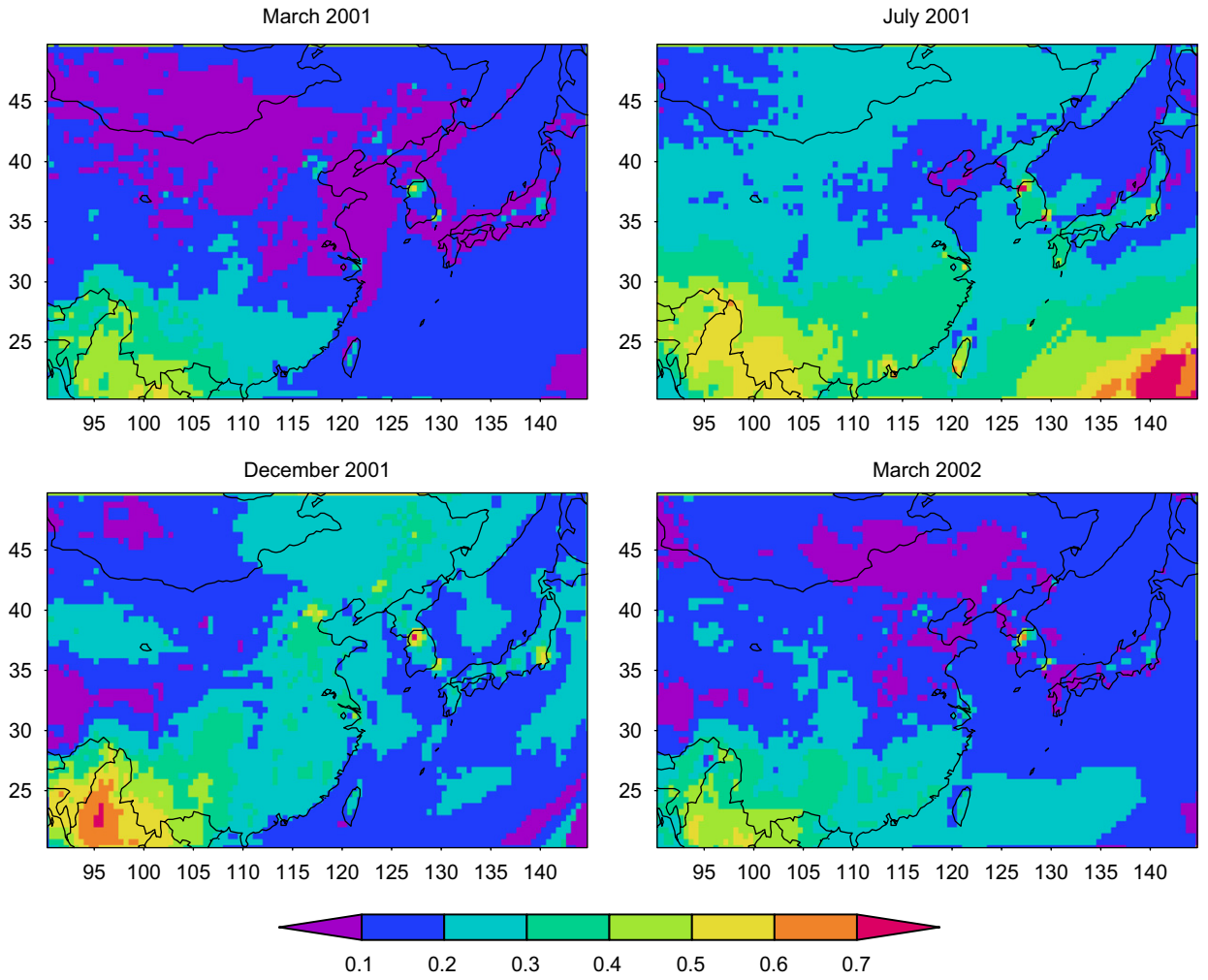

Fig. 12. The coefficient of variation (CV) for monthly mean near surface ozone, defined as the standard deviation of the modeled fields divided by the average, for the different seasons.

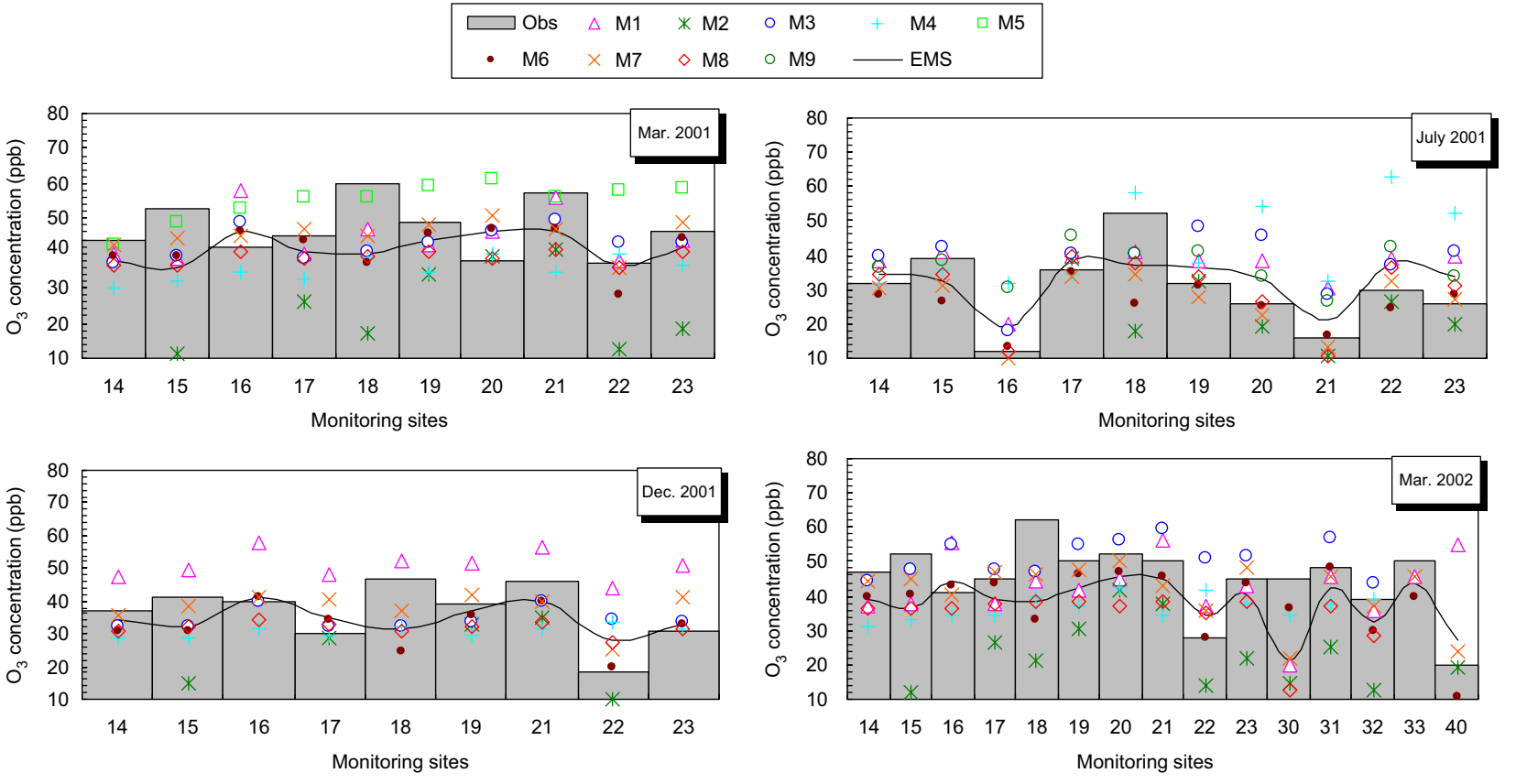

Fig. 13. The predicted and observed monthly mean near surface ozone concentrations over Japan. The locations of the observations sites are given in Fig. 1. Also shown is the ensemble mean prediction (EMS).

5. Summary

The MICS-Asia Phase II study examined four different periods, encompassing two different years and three different seasons. Nine different regional modeling groups simulated chemistry and transport of O_3, aerosols, acid deposition, and related precursors using common emissions and boundary conditions derived from the MOZART global CTM. Model predictions were compared with each other, and with measured concentration and deposition data provided by the recently established EANET monitoring program.

Comparison with monthly averaged and daily observations demonstrate that collectively the current generation of CTMs is capable of representing many of the main features of the distributions of trace gases, aerosols, and acid deposition in East Asia. The performance of the CTMs in East Asia is similar to the performance of the models (and other models) when applied to the other regions (McKeen et al., 2005).

There were also significant differences between the predictions from the various models, and these were associated with differences in the details of the model formulation, including parameterizations and numerical methods. For example, the variability of predicted aerosol nitrate due to different aerosol parameterizations tested in a single CTM was found to be as large as the variability among the different CTMs, taking into account all model differences. These results suggest that a quantitative attribution of the causes of differences between the model predictions will require further sensitivity tests to isolate individual processes (e.g., advection, deposition).

The results from this study also suggest directions for future model development. For example, most of the dry deposition schemes used in the CTMs were developed in USA/Europe and their parameterizations (e.g., seasonal categories, land use information, etc.) may not be suitable for the Asian region. The further development and testing of parameterizations for Asia is needed. Boundary conditions are another important source of uncertainty in regional predictions in Asia. Driving regional CTMs with boundary conditions from global models tend to improve model performance, and also provide more realistic spatial and temporal variability. However, the global CTMs are themselves uncertainty, so improvements in model performance will require reducing the uncertainties in the boundary conditions. The demand to reduce model uncertainty has important implications for the observational network. In general, the performance of the CTMs was better over Japan than over other regions. This is due in part to the location of Japan within the modeling domain, and to the high density of measurements over Japan. In the western portion of the domain, there are few measurement sites. EANET has plans to expand the monitoring network, especially for western region in China.

Finally an understanding of S/R relationships at regional and hemispheric scales is important in establishing effective emission management strategies. As S/R relationships are often estimated using CTMs, it is important to evaluate the uncertainty in predicted S/R relationships. In MICS-I, we focused on the intercomparison of predicted S/R relationships for sulfur deposition. However, it is now recognized that S/R for aerosol and O_3 are important in evaluating the contributions of local, regional, and distant (hemispheric) sources. Recently, an intercomparison study of S/R relationships at hemispheric scales has been initiated by the task force on hemispheric transport of air pollution (as part of the convention on long-range transport of air pollution), using global CTMs (www.htap.org). These global scale studies will be useful for assessing regional air quality, but they do not replace the need for regional scale analysis. Regional models are needed to estimate S/R relationships at regional scales, and to examine pollution and precursor outflow to other areas. These regional scale analyses also contribute to greater understanding of local air pollution problems, a major problem for the rapidly growing megacities in Asia. Clearly, links are needed to connect air quality mechanisms across global, regional, and urban scales. We plan to extend the MICS study to include such topics in the future.

References

ADORC, 2003. MICS-Asia Phase II–A Model Intercomparison Study in Asia 〈http://www.adorc.gr.jp/adorc/mics.html〉.

Berge, E., 1993. Coupling of wet scavenging of sulphur to clouds in a numerical weather prediction model. Tellus 45B, 1–22.

Boutahar, J., Lacour, S., Mallet, V., Quélo, D., Roustan, Y., Sportisse, B., 2004. Development and validation of a fully modular platform for numerical modelling of air pollution: Polair3D. International Journal of Environmental Pollution 22, 17–18.

Carmichael, G., Calori, G., Hayami, H., Uno, I., Yeon Cho, S., Engardt, M., Kim, S.-B., Ichikawa, Y., Ikeda, Y., Woo, J.H.,

Ueda, H., Amann, M., 2001. A brief overview of the model intercomparison study for long range transport models in East Asia. Water, Air, and Soil Pollution 8 (Special Issue for Acid Rain 2000).

Carmichael, G.R., Calori, G., Hayami, H., Uno, I., Cho, S.Y., Engardt, M., Kim, S.-B., Ichikawa, Y., Ikeda, Y., Woo, J.-H., Ueda, H., Amann, M., 2002. The MICS-Asia study: model intercomparison of long-range transport and sulfur deposition in East Asia. Atmospheric Environment 36, 175–199.

Carmichael, G.R., Tang, Y., Kurata, G., Uno, I., Streets, D., Woo, J-H., Huang, H., Yienger, J., Lefer, B., Shetter, R., Blake, D., Atlas, E., Fried, A., Apel, E., Eisele, F., Cantrell, C., Avery, M., Barrick, J., Sachse, G., Brune, W., Sandholm, S., Kondo, Y., Singh, H., Talbot, R., Bandy, A., Thorton, D., Clarke, A.D., Heikes, B., 2003. Regional-scale chemical transport modeling in support of the analysis of observations obtained during the TRACE-P Experiment. Journal of Geophysical Research 108 (D21), 8823.

Chang, L.S., Park, S.U., 2004. Direct radiative forcing due to anthropogenic aerosols in East Asia during April 2001. Atmospheric Environment 38, 4467–4482.

Chang, J.S., Brost, R.A., Isaksen, I.S.A., Madronich, S., Middleton, P., Stockwell, W.R., Walcek, C.J., 1987. A three-dimensional Eulerian acid deposition model: physical concepts and formulation. Journal of Geophysical Research 92, 14681–14700.

Dentener, F., Drevet, J., Lamarque, J.F., Bey, I., Eickhout, B., Fiore, A.M., Hauglustaine, D., Horowitz, L.W., Krol, M., Kulshrestha, U.C., Lawrence, M., Galy-Lacaux, C., Rast, S., Shindell, D., Stevenson, D., Van Noije, T., Atherton, C., Bell, N., Bergman, D., Butler, T., Cofala, J., Collins, B., Doherty, R., Ellingsen, K., Galloway, J., Gauss, M., Montanaro, V., Müller, J.F., Pitari, G., Rodriguez, J., Sanderson, M., Strahan, S., Schultz, M., Solmon, F., Sudo, K., Szopa, S., Wild, O., 2006. Nitrogen and sulphur deposition on regional and global scales: a multi-model evaluation. Global Biogeochemical Cycles GB4003.

EANET, 2001. Data Report on the Acid Deposition in the East Asian Region 2001, available at 〈http://www.eanet.cc/product.html〉.

EANET, 2002. Data Report on the Acid Deposition in the East Asian Region 2002, available at 〈http://www.eanet.cc/product.html〉.

EANET, 2003. Technical Document for Filter Pack Method in East Asia. 〈http://www.eanet.cc/product/techdoc_fp.pdf〉.

Engardt, M., 2000. Sulphur simulations for East Asia using the match model with meteorological data from ECMWF. RMK No. 88, Swedish Meteorological and Hydrological Institute, 33pp.

European Space Agency, 2004. ATSR World Fire Atlas, ESA/ESRIN, Frascati, Italy, available at 〈http://dup.esrin.esa.int/ionia/wfa/index.asp〉.

Fu, J., Jang, C.C., Streets, D.G., Li, Z., Kwok, R., Han, Z. MICS-ASIA II: Modelling gaseous pollutants and evaluating an advanced modeling system over East Asia. Atmospheric Environment 42, 3571–3583.

Grell, G.A., Dudhia, J., Stauffer, D.R., 1994. Description of the fifth generation Penn State/NCAR meso-scale model (MM5). NCAR Technical Note, NCAR/Tn-398 + STR.

Han, Z.W., Ueda, H., Matsuda, K., Zhang, R.J., Arao, K., Kanai, Y., Hasome, H., 2004. Model study on particle size segregation and deposition during Asian dust events in March 2002. Journal of Geophysical Research 109.

Han, Z., Sakurai, T., Ueda, H., Matsuda, K., Hozumi, Y., Carmichael, G.R., Streets, D., Park, S.U., Fung, C., Chang, A., Kajino, M., Thongboonchoo, N., Engardt, M., Bennet, C., Hayami, H., Sartelet, K., Holloway, T., Wang, Z., Amann, M., 2008. Companion paper. MICS-ASIA II: Model intercomparison and evaluation of ozone and relevant species. Atmospheric Environment 42, 3491–3509.

Hayami, H., 2005. Behavior of secondary inorganic species in gaseous and aerosol phases measured in Fukue Island, Japan, in dust season. Atmospheric Environment 39, 2243–2248.

Hayami, H., Sakurai, T., Matsuda, K., Han, Z., Ueda, H., Carmichael, G.R., Streets, D., Holloway, T., Wang, Z., Thongboonchoo, N., Engardt, M., Bennet, C., Fung, C., Chang, A., Park, S.U., Kajino, M., Amann, M., 2008. Companion paper. MICS-ASIA II: Model intercomparison and evaluation of particulate sulfate, nitrate and ammonium. Atmospheric Environment 42, 3510–3527.

Holloway, T., et al., 2008. MICS-ASIA II: Impact of global emissions on regional air quality in Asia. Atmospheric Environment 42, 3543–3561.

Horowitz, L.W., Walters, S., Mauzerall, D.L., Emmons, L.K., Rasch, P.J., Granier, C., Tie, X., Lamarque, J.-F., Schultz, M.G., Tyndall, G.S., Orlando, J.J., Brasseur, G.P., 2003. A global simulation of tropospheric ozone and related tracers: description and evaluation of MOZART, version 2. Journal of Geophysical Research 108 (D24), 4784.

Ichikawa, Y., Fujita, S., 1995. An analysis of wet deposition of sulfate using a trajectory model for East Asia. Water, Air, and Soil Pollution 85, 1921–1926.

Jacob, D., Crawford, J., Kleb, M., Conners, V., Bendura, R., Raper, J., Sachse, G., Gille, J., Emmons, L., 2003. The transport and chemical evolution over the Pacific (TRACE-P) mission: design, execution, and overview of first results. Journal of Geophysical Research 108 (D20), 8781.

Kajino, M., Ueda, H., Satsumabayashi, H., An, J., 2004. Impacts of the eruption of Miyakajima volcano on air quality over Far East Asia. Journal of Geophysical Research 109, D21204.

Kannari, A., Streets, D.G., Tonooka, Y., Murano, K., Baba, T., 2008. MICS-ASIA II: An inter-comparison study of emission inventories for the Japan region. Atmospheric Environment 42, 3584–3591.

Kazahaya, K., 2001. Volcanic gas study of the (2000) Miyakejima volcanic activity: degassing environment deduced from adhered gas component on ash and SO_2 emission rate. Journal of Geography 110 (2), 271–279 (in Japanese).

McKeen, S., Wilczak, J., Grell, G., Djalalova, I., Peckham, S., Hsie, E.-Y., Gong, W., Bouchet, V., Menard, S., Moffet, R., McHenry, J., McQueen, J., Tang, Y., Carmichael, G.R., Pagowski, M., Chan, A., Dye, T., 2005. Assessment of an ensemble of seven real-time ozone forecasts over Eastern North America during the summer of 2004. Journal of Geophysical Research 110, D21307.

Pielke, R.A., et al., 1992. A comprehensive meteorological modeling system-RAMS. Meteorology and Atmospheric Physics 49, 69–91.

Sartelet, K.N., Hayami, H., Sportisse, B., 2008. MICS Asia Phase II—Sensitivity to the aerosol module. Atmospheric Environment 42, 3562–3570.

Seinfeld, J.H., 1986. Atmospheric Chemistry and Physics of Air Pollution. Wiley, New York, p. 738.

Streets, D.G., et al., 2003a. An inventory of gaseous and primary emissions in Asia in the year 2000. Journal of Geophysical Research 108 (D21), 8809.

Streets, D.G., Yarber, K.F., Woo, J.-H., Carmichael, G.R., 2003b. Biomass burning in Asia: annual and seasonal estimates and atmospheric emissions. Global Biogeochemical Cycles 17 (4), 1099.

Streets, D.G., Bond, T.C., Carmichael, G.R., Fernandes, S.D., Fu, Q., He, D., Klimont, Z., Nelson, S.M., Tsai, N.Y., Wang, M.Q., Woo, J.-H., Yarber, K.F., 2003c. An inventory of gaseous and primary aerosol emissions in Asia in the year 2000. Journal of Geophysical Research 108 (D21), 8809.

Wang, Z., et al., 2008. MICS-ASIA II: Model inter-comparison and evaluation of acid deposition. Atmospheric Environment 42, 3528–3542.

Wesely, M.L., 1989. Parameterization of surface resistances to gaseous dry deposition in regional-scale numerical models. Atmospheric Environment 23, 1293–1304.

Woo, J.-H., et al., 2003. Contribution of biomass and biofuel emissions to trace gas distributions in Asia during the TRACE-P experiment. Journal of Geophysical Research 108 (D21), 8812.